

# Solid state sulfide Based LI-Metal batteries for EV applications

## D4.5 Report on monolayer pouch cell assembly

Paul Wulfert-Holzmann, Sabrina Zellmer  
Fraunhofer IST

Mattis Batzer  
TU Braunschweig (linked third party)



<b>Deliverable No.</b>	SUBLIME D4.5	
<b>Related WP</b>	WP4	
<b>Deliverable Title</b>	Report on monolayer pouch cell assembly	
<b>Deliverable Date</b>	30.06.2023	
<b>Deliverable Type</b>	REPORT	
<b>Dissemination level</b>	Public (PU)	
<b>Written By</b>	Paul Wulfert-Holzmann (Fraunhofer) Mattis Batzer (TU Braunschweig)	2023-05-12
<b>Checked by</b>	Pedro Lopez (CICe)	2023-05-24
<b>Reviewed by (if applicable)</b>	Pedro Lopez (CICe) Alexander Beutl (AIT)	2023-05-24 2023-06-22
<b>Approved by</b>	Seyedhosein Payandeh (FEV)	2023-06-28
<b>Status</b>	Draft 1.0 / Draft 2.0 / <b>Final</b>	2023-06-14

## Disclaimer / Acknowledgment



Copyright ©, all rights reserved. This document or any part thereof may not be made public or disclosed, copied or otherwise reproduced or used in any form or by any means, without prior permission in writing from the SUBLIME Consortium. Neither the SUBLIME Consortium nor any of its members, their officers, employees or agents shall be liable or responsible, in negligence or otherwise, for any loss, damage or expense whatever sustained by any person as a result of the use, in any manner or form, of any knowledge, information or data contained in this document, or due to any inaccuracy, omission or error therein contained.

All Intellectual Property Rights, know-how and information provided by and/or arising from this document, such as designs, documentation, as well as preparatory material in that regard, is and shall remain the exclusive property of the SUBLIME Consortium and any of its members or its licensors. Nothing contained in this document shall give, or shall be construed as giving, any right, title, ownership, interest, license or any other right in or to any IP, know-how and information.

This project has received funding from the European Union's Horizon 2020 research and innovation programme under grant agreement No 875028. The information and views set out in this publication does not necessarily reflect the official opinion of the European Commission. Neither the European Union institutions and bodies nor any person acting on their behalf, may be held responsible for the use which may be made of the information contained therein.

## Publishable summary

The deliverable D4.5 “Report on monolayer pouch cell assembly” focuses on the assembly of all-solid-state monolayer pouch cells within the frame of Work Package 4 and Task 4.4. It is connected to Task 4.3 in which different process routes for the fabrication of cathode and separator components have been evaluated, i.e. dry processing, infiltration, wet coating and extrusion. Of those four processes, the extrusion route has been identified as the most promising choice in terms of throughput, material performance, quality and scalability. For further details, please refer to deliverable D4.4 “Report on layer processing towards upscaling”.

In the present deliverable, the components from the extrusion route described in Task 4.3 are applied for the pouch cell assembly. They are based on the SUBLIME Gen IV electrolyte, and NCM 811 as cathode active material. As anode material, a Lithium/Indium combination is applied. Comprising a capacity of approximately  $2.8 \text{ mAh cm}^{-2}$ , monolayer pouch cells with an electrode size of  $3 \times 3 \text{ cm}^2$  and therefore a total capacity of 25.7 mAh are prepared.

The preparation comprises the following steps: First, for the anode, a Lithium/Copper foil as well as an Indium foil are punched and subsequently stacked together to form a Lithium/Indium bilayer that later results in the desired LiIn alloy providing a better stability against sulfidic solid-state electrolytes than pure Lithium as anode material<sup>1</sup>. In addition, a composite cathode/separator bilayer is punched out. Here, an excess area takes into account a possible spreading of the anode material during pressurization. After punching, the cathode/separator bilayer is compacted at a pressure of 145 MPa using a hydraulic press. Next, electrode tabs are welded to the aluminium and copper current collectors using ultrasonic welding to provide for the electrical contact. Finally, the components are stored and sealed in a pouch bag. Due to the reactive nature of all components in ambient air, all processes are performed in a glovebox (punching, stacking) or dry room (electrode welding).

For a first assessment of the electrochemical performance, five pouch cells were cycled at 25 °C with a C-rate of 0.02C and an external pressure of 10 MPa. The specific discharge capacities obtained from the  $3 \times 3 \text{ cm}^2$  pouch cells were compared to the performance in Teflon tube tests (circular samples of 16 mm diameter) applied within Task 4.3 and Deliverable 4.4. The latter were cycled at an external pressure of 25 MPa, which due to mechanical specifications of the cell press device was not feasible for the larger pouch cells. It was found that the specific discharge capacities were significantly lower for the  $3 \times 3 \text{ cm}^2$  pouch cells than for the cells cycled in the Teflon tube. Since the same materials were applied for both tests, this might be explained with a reduced external pressure resulting in poorer contact between the components. However, recent literature<sup>2</sup> also suggests a significant impact of initial fabrication pressure on the cycling performance of all-solid-state batteries, rather than only focusing on the stack pressure. Therefore, to explain the reduced specific discharge capacities further investigations are necessary as will be performed within WP6.

In total, this report shows the successful fabrication of monolayer all-solid-state pouch cells with a size of  $3 \times 3 \text{ cm}^2$  and, using the currently available cathode layers, a capacity of approximately 25 mAh. It summarizes the relevant process steps for the fabrication of cathode and separator layers and identifies the steps during the pouch cell assembly. With that, the milestone MS04 “Pouch cells (up to 40 mAh) assembled has been achieved.

---

<sup>1</sup> Santosha et al., Batteries & Supercaps 2019, 2, 524–529,

<https://doi.org/10.1002/batt.201800149>

<sup>2</sup> Doux et al., J. Mater. Chem. A, 2020, 8, 5049–5055, <https://doi.org/10.1039/C9TA12889A>

# Contents

1	Introduction .....	6
2	Methods and Results .....	7
2.1	Material, Processes and Analysis.....	7
2.1.1	Material .....	7
2.1.2	Processes .....	7
2.1.3	Analysis.....	7
2.2	Cell manufacturing .....	8
2.3	Cycling data .....	10
2.4	Challenges during pouch cell assembly.....	12
3	Discussion and Conclusions .....	12
4	Risk register.....	14
5	Acknowledgement .....	15
6	Appendix A – Quality Assurance.....	<b>Error! Bookmark not defined.</b>

## List of Figures

Figure 1: a) Format of anodes and cathodes. b) Punching dies. c) Cathode + separator bilayers and anode samples. d) Hydraulic press. .... 9

Figure 2: a) Uncontacted stack of cathode and anode. b) Electrodes after ultrasonic welding of tabs. c) Ultrasonic welding device. d) As-assembled pouch cell. .... 10

Figure 3: a) Sketch of the experimental setup and the application of an external pressure on the pouch cell. b) Cell press device including fiberglass cylinders and pouch cell. c) Specific discharge capacity and columbic efficiency of pouch cells. d) U-Q-curves for the 1<sup>st</sup>, 3<sup>rd</sup> and 5<sup>th</sup> cycle. e) dQ/dV-curves for the 1<sup>st</sup>, 3<sup>rd</sup> and 5<sup>th</sup> cycle. .... 11

Figure 4: Representative cycling results of identical components but characterized in PTFE cylinder assembly, as reported in D4.4, i.e. f) specific discharge capacities and Coulombic efficiency and g) U-Q-curves for the 1st, 3rd and 5th cycle. .... 12

## List of Tables

Table 1: Properties of final separators and cathodes (reported in D4.4). .... 12

Table 2: Specific capacity for PTFE- and Pouch Cell Setup ..... 13

Table 3: Risk Register ..... 14

Table 4: Project Partners ..... 15

SYMBOL	SHORTNAME
t	Time
Q	Charge amount
E	Voltage

# 1 Introduction

This deliverable addresses the assembly of solid-state, Lithium-ion monolayer pouch cells. It is connected to Task 4.4 “Monolayer pouch cell assembly” in Work Package 4 and establishes a connection between the process evaluation for the preparation of solid-state battery components in Task 4.3, i.e. composite cathodes and solid-state electrolyte layers, and their electrochemical characterization in Work Package 6. In Task 4.3, different process routes have been evaluated and reported in Deliverables 4.3 and 4.4, including dry processing, infiltration, wet coating and extrusion. The extrusion process has been identified as the most feasible route in terms of performance, throughput and scalability. Cathode and solid-state electrolyte layers have thereafter been prepared on a laboratory scale, using NCM 811 and the sulfide electrolyte developed within the project (Work Package 3).

In Task 4.4, these components are assembled into monolayer pouch cells and transferred to WP6 for electrochemical testing. The task foresees the production of pouch cells with up to 40 mAh capacity. As the cathodes have an areal capacity of approximately  $2.8 \text{ mAh cm}^{-2}$ , the resulting pouch cells exhibit a capacity of 25 mAh. Both the process steps for producing the cathode and separator layers and the cell construction steps are almost exclusively transferable to size-independent cells. The only exceptions are compaction using a hydraulic press, which will be replaced by a calender in the medium term, and the pressure during cyclization. The latter requires the use of larger cell press devices.

In addition to the above mentioned aspects, Task 4.4 aims at the provision of pouch cells for the primary and secondary pathway, i.e. with objectives of 450 Wh/kg and 1200 Wh/L (primary) and a power density of 5 kW/kg during peak discharge as well as a high charge current rate of 5C (secondary pathway). Given the preliminary test results presented in the following report, these goals will probably not be met with the currently available materials and components, though a final assessment will only be possible after extensive testing by project partners in WP6. Based on information from the project partners, new and improved cathode active material and solid electrolyte will be available within the next months. Once provided, new components with presumably better electrochemical performance in the frame of primary and secondary pathway can be prepared with the extrusion process described in D4.4.

## 2 Methods and Results

### 2.1 Material, Processes and Analysis

#### 2.1.1 Material

The cathode layers used for the pouch cells contained three powders and a polymer-based binder: NCM 811 by Umicore N.V./S.A. as an active material, sulfide electrolyte from Solvay S.A. and carbon black of type Super C65 procured from Timcal Ltd. as a conductive additive. The binder was hydrogenated nitrile-butadiene-rubber (HNBR) of type Therban AT LT 04 provided by Arlanxeo Deutschland GmbH. The formulation is 71.23 wt.% active material, 23.74 wt.% solid electrolyte, 2.00 wt.% conductive additive and 3.03 wt.% binder. The separator layers only contained solid electrolyte and binder, but the manufacturers and types of material were identical to those of the cathode layers. The formulation contained 97.00 wt.% solid electrolyte and 3.00 wt.% binder. Cathode and separator suspensions were prepared with a solvent content of 40 wt.% p-xylene purchased from Carl Roth GmbH & Co. KG. While the cathode suspension was coated on aluminum substrate (15  $\mu\text{m}$  film thickness, Hydro Aluminium Rolled Products GmbH & Co. KG), the separator was applied directly to the cathode layer. Lithium coated on copper substrate (10  $\mu\text{m}$  Cu, 60  $\mu\text{m}$  Li, Honjo Chemical Corp.) and additionally an indium anode (127  $\mu\text{m}$ , Alfa Aesar by Thermo Fisher Scientific Inc.) were used as anode. The current collectors were connected with nickel conductive taps from Targray Technology International Inc.

#### 2.1.2 Processes

The process chain for the production of the composite cathodes started with the dry mixing of the powder components in an intensive mixer (Eirich EL1, Gustav Eirich GmbH & Co. KG). The powder was added in three steps: 1<sup>st</sup> half of the conductive additive and solid electrolyte, 2<sup>nd</sup> active material, 3<sup>rd</sup> half of the conductive additive. After the powder additions, dry dispersion of the material was carried out with a tool speed of 15  $\text{m s}^{-1}$  and a counter-, slowly rotating container. The powder filling level was 50 vol.%, and a pin-whirler was used as the dispersing tool. The powder was then processed into a suspension using a Process 11 Hygienic TSE twin-screw extruder from Thermo Fisher Scientific Inc. The parameters were obtained from Task 4.3, recently reported in Deliverable 4.4 (600  $\text{min}^{-1}$ , 40  $^{\circ}\text{C}$ , 360  $\text{g h}^{-1}$ ). The pre-mixed powder was fed gravimetrically and the HNBR binder, previously dissolved in p-xylene, was fed volumetrically into the extruder and dispersed by the screws. The suspension, which is conveyed through a round strand die, was collected and coated onto the aluminum substrate using doctor blade technology (gap width 300  $\mu\text{m}$ ) and a film applicator (COATMASTER 510, Erichsen GmbH & Co. KG). The feed rate was 0.6  $\text{m min}^{-1}$  and the temperature of the plate was 25  $^{\circ}\text{C}$ . After the cathode layers (approx. 6 x 25  $\text{cm}^2$ , 40 pieces per experiment limited by the storage inside the glovebox) have dried, the separator was coated directly onto the cathode. The wet dispersion step was carried out with different parameters (100  $\text{min}^{-1}$ , 40  $^{\circ}\text{C}$ , 480  $\text{g h}^{-1}$ ) and the dry mixing step was omitted, since only the solid electrolyte was in powder form. The coating, on the other hand, was applied with a doctor blade gap width of 500  $\mu\text{m}$ . Subsequently, square cathode and separator samples with an edge length of 30 mm (not including the electrode flags) were cut out, compacted with a pressure of 145 MPa in a hydraulic press (PW 10, Paul-Otto Weber GmbH) and transferred to the pouch cell assembly. All processes have been carried out in gloveboxes under inert-gas atmosphere, except dry mixing (approximately 15 minutes exposition including mixing and sample transfer) and welding of conductor tabs to the electrodes of the pouch cell (approximately 10 minutes including welding and sample transfer). These steps were performed in a dry room with a dew point of -35  $^{\circ}\text{C}$ .  $\text{H}_2\text{S}$  exposure was only measured when the mixer was filled with solid electrolyte; it was 5 ppm. In the following mixing process as well as in the welding step there is no measurable exposure.

#### 2.1.3 Analysis

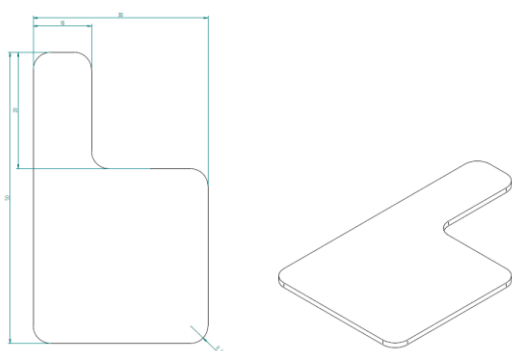
To characterize the pouch cells, some properties of the cathode and separator layers were determined: The mass loading of the cathodes plays a major role in calculating the rated capacity for cycling of the

cells; this was determined gravimetrically. Likewise, the porosity was determined mathematically from the mass loading and the layer thickness. These steps were carried out analogously for the separator layers. Furthermore, the adhesive strength of both components and the electrical conductivity of the cathodes were determined (tensile testing machine Z020, Roell Zwick GmbH). These represent production-relevant parameters, e.g. with regard to roll-to-roll coating and doctoring of the separator layer onto the cathode layer or electrical contacting of the active material particles. In addition, the ionic conductivity of the separator layer and the electrochemical resistance of the cathode layer were determined by means of electrochemical impedance spectroscopy. This was done on a ZAHNER Zennium Pro from ZAHNER-Elektrik GmbH & Co. KG in a frequency range of 100 mHz - 4 MHz at a voltage amplitude of 10 mV. Separators coated on aluminum or coated symmetrical cathode cells were measured in the standardized Teflon cell at a measuring pressure of 25 MPa as well as a temperature of 25 °C. Finally, pouch cells with a total area of 3x3 cm<sup>2</sup> aiming at a capacity of 25 mAh were cycled. The existing equipment for punching the samples and for pressing (compaction for manufacturing and cycling) is designed for 9 cm<sup>2</sup> cells and therefore responsible for not reaching the originally specified 40 mAh. Otherwise, 40 mAh could only have been achieved with a higher surface loading, which in turn probably lowers the cell performance. However, larger formats are possible in principle by modifying the equipment. The procedure involved five cycles at a C-rate of 0.02C in a voltage range between 3.8 and 2.2 V. The cycling was performed with the aid of a cell press device (measuring pressure 25 MPa) in a climatic cabinet that ensures a constant temperature of 25 °C. All analysis methods have been carried out in gloveboxes under inert-gas atmosphere, except adhesive and electrical testing. These steps were performed in a dry room with a dew point of -35 °C.

## 2.2 Cell manufacturing

Following the steps mentioned in section 2.1.2 for the production of cathode and separator layers, the pouch cells were assembled. For this purpose, anodes were first punched out, both, from an indium layer and a lithium layer deposited on copper. They had a square shaped base (see Figure 1a) and formed the basis of the pouch cells. Subsequently, a likewise square shape was punched out of the separator/cathode double layer. Its edge length was slightly larger than that of the anode in order to prevent a short circuit due to the spreading of the anode material caused by pressing of the pouch cells while cycling. The anode and cathode layers were punched out using the tools shown in Figure 1b. After punching, the particulate bilayer was compacted. Compared with the cells based on the PTFE cell produced for Deliverable 4.4, however, a lower pressure of 145 MPa in contrast to 400 MPa had to be used, since the maximum compaction force of the hydraulic press (compare Figure 1d) was limited to 130 kN due to the surface area being 4.5 times higher.

a)



b)



c)



d)



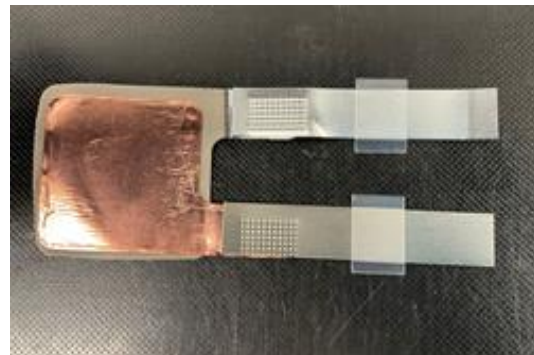
Figure 1: a) Format of anodes and cathodes. b) Punching dies. c) Cathode + separator bilayers and anode samples. d) Hydraulic press.

This was followed by stacking the double layer for the cathode and separator, or the indium and lithium on copper layer on the anode side (see Figure 2a). Further compaction of the anode onto the particulate layers did not happen. The cell components were provisionally sealed for transport from the glovebox to the dry room. In the dry room, the pouch was opened again and nickel conductor tabs were provisionally taped on a base plate in order to be connected to the arrester flags of the aluminum and copper substrates (compare Figure 2b). After attaching the nickel tabs using an ultrasonic welder (see Figure 2c) in the drying room, the cells were sealed under reduced pressure in pouch foil within Argon atmosphere (compare Figure 2).

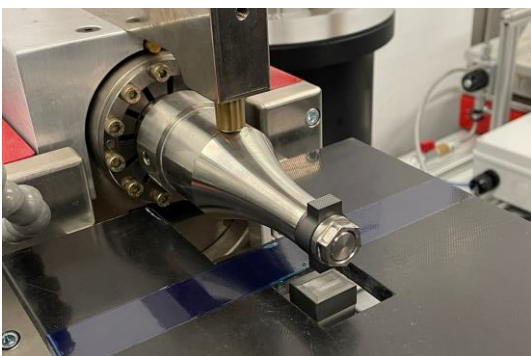
a)



b)



c)



d)



Figure 2: a) Uncontacted stack of cathode and anode. b) Electrodes after ultrasonic welding of tabs. c) Ultrasonic welding device. d) As-sembled pouch cell.

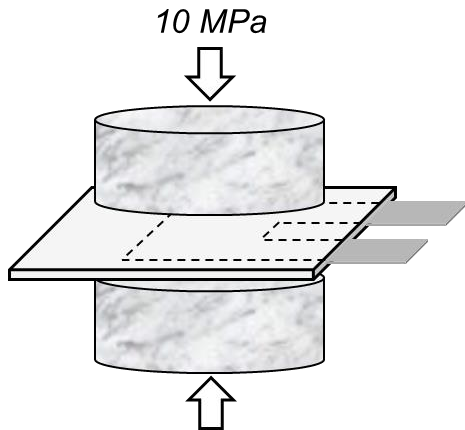
## 2.3 Cycling data

For electrochemical characterization of the assembled pouch cells and especially the application of an external pressure, the previously reported cell press devices (previously used for circular samples in a PTFE measurement cell) were used with special inserts. Figure 3a shows the pouch cell between two cylindrical inserts. The pouch cell and incompressible fiberglass cylinders are inserted between the middle and lower plates of the cell press and a force is applied as via a trapezoidal threaded spindle. Due to the larger surface area of the cell, a lower pressure compared to the circular samples of previous measurements could be applied (analogous to section 2.2). While for the circular samples a pressure of up to 25 MPa could be applied, the pressure for the pouch cells was reduced to 10 MPa. For each measurement, five cycles with a C-rate of 0.02C were performed.

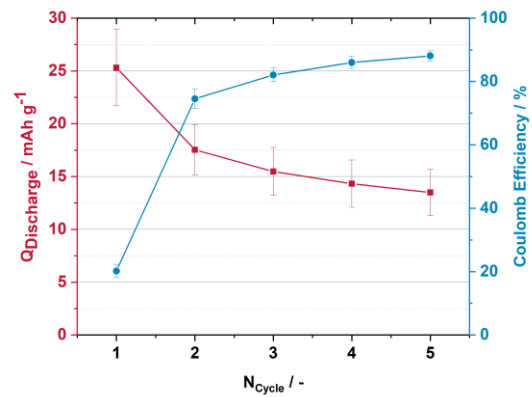
Figure 3c shows the specific capacity averaged from five pouch cells and their Coulombic efficiency: starting from 19 mAh g<sup>-1</sup> in the 1<sup>st</sup> cycle, the specific capacity drops to 10 mAh g<sup>-1</sup> by the 5<sup>th</sup> cycle. In parallel, the Coulombic efficiency increases from 17 % in the 1<sup>st</sup> cycle to 85 % in the 5<sup>th</sup> cycle. It is thus only one fifth of the capacity originally achieved in Deliverable 4.4 with the use of the PTFE cylinder assembly (112 mAh g<sup>-1</sup>) and only 9 % of the nominal capacity of the active material (218 mAh g<sup>-1</sup>) – representative results are again displayed in Figure 4 and Table 2. Part of the capacity loss can be attributed to the changed compression and measurement parameters: While a pressure of 400 MPa could be applied during the fabrication process of the previous cells in the 16 mm PTFE cylinder (Deliverable 4.4), only a third of the pressure could be applied here due to the larger area of the pouch cell (see section 2.2) and the torque limitation of the cell press device. This results in higher porosity, which reduces both the electronic and ionic conductivity within the cathode and separator layer, respectively, as well as the volumetric energy density. Due to the reduction of the pressure during the cycling of the cell from 25 to 10 MPa, the contact between the electrodes and the separator layer might decrease as well, which in turn increases the interfacial resistances and thus lowers the conductivities.<sup>3</sup> In addition to the different compression, the probability of defects in the electrode and separator also grows with the increased sample area. Although all five assembled pouch cells worked correctly, i.e. there was no defect in the separators that could have caused a short circuit, deviating layer thicknesses in the cathode or heterogeneously dispersed soot or solid electrolyte particles cannot be ruled out. This would result in a lower mass loading, which again would result in inhomogeneous current distributions or locally poorly bound active material particles. Figure 3d shows that the capacity initially drops sharply from the 1<sup>st</sup> to the 3<sup>rd</sup> cycle and then only slightly until the 5<sup>th</sup> cycle. Furthermore, the final capacity at the lower voltage limit deviates from the value given in figure 3c, which can be explained by the blanking of the constant current step during the discharge process. Possible reasons for the strong capacity loss are overpotentials or the loss of active material due to irreversible electrochemical reactions. To test this assumption, the differential capacitance curves of the three selected cycles are shown in Figure 3e. While the absolute value dQ/dE first drops sharply, then slightly, with increasing cycle number, analogous to Figure 3d, the peak remains at about 2.7 V. This indicates that the active material is lost due to irreversible electrochemical reactions and that the main reason for the capacitance degradation in Figure 3c is a contact loss of the active material.

<sup>3</sup> Batzer et al., *Materials Today Communications* 30 (2022) 103189, <https://doi.org/10.1016/j.mtcomm.2022.103189>

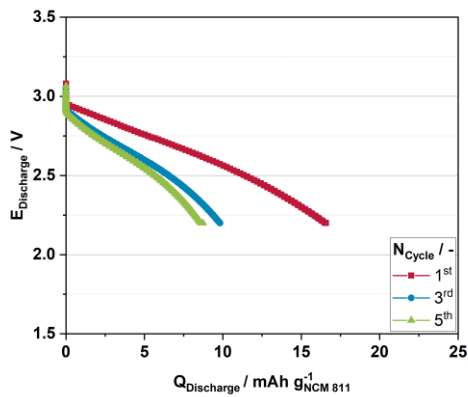
a)



b)



c)



d)

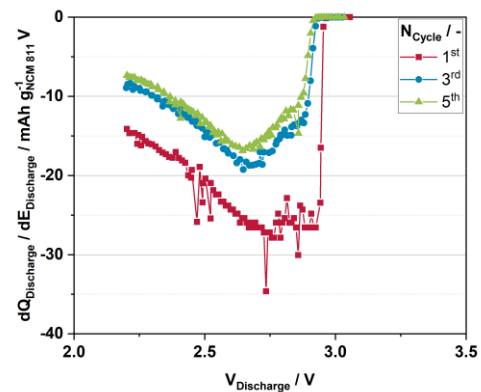
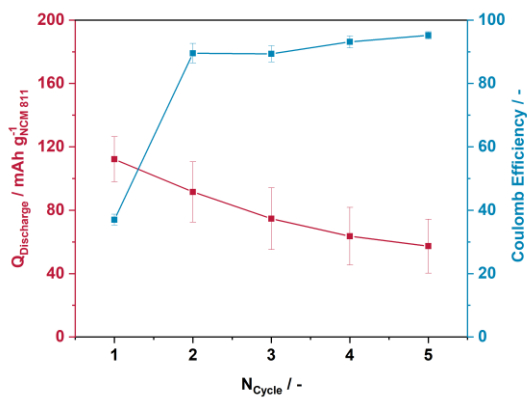


Figure 3: a) Sketch of the experimental setup and the application of an external pressure on the pouch cell. b) Specific discharge capacity and coulombic efficiency of pouch cells. c) E-Q-curves for the 1<sup>st</sup>, 3<sup>rd</sup> and 5<sup>th</sup> cycle. d) dQ/dE-curves for the 1<sup>st</sup>, 3<sup>rd</sup> and 5<sup>th</sup> cycle.

a)



b)

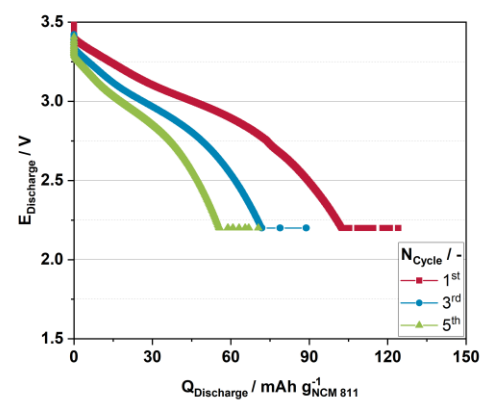


Figure 4: Representative cycling results of identical components but characterized in PTFE cylinder assembly, as reported in D4.4, i.e. a) specific discharge capacities and Coulombic efficiency and b) E-Q-curves for the 1st, 3rd and 5th cycle.

## 2.4 Challenges during pouch cell assembly

The challenges in the construction of pouch cells arise primarily from the considerably increased sample area. They relate both to the higher probability of defects (heterogeneous particle distribution, non-uniform mass loading) as well as the physical challenges involved in compacting the layer (force increases linearly with area, otherwise lower porosity, conductivity and higher interfacial resistances). In addition, there are defects that result from the manual process of pouch cell assembly: For example, the particulate layers become wavy and partially detach from the substrate both as a result of compaction with the aid of the pouch cell and during initial trials with the calender. This makes further processing of the layers, such as die cutting and stacking, more difficult. There is still a risk that the arrester flags of the substrates (small, rounded rectangles above the actual electrode surface) can be torn off during pressing, when welding the nickel arresters or when connecting the cell to the battery tester. Finally, when anode, separator and cathode are not well aligned, the electrochemical performance could be deteriorated and there could even be short circuits due to contact between anode and cathode. Therefore, careful handling and processing is vital. It would also be possible to use an isostatic press: By applying pressure uniformly through a fluid from all sides to the welded layers or the cell, high pressure can be applied gently. Although this is not a scalable method, it would be conceivable as a preliminary option.

## 3 Discussion and Conclusions

In Table 1, the properties determined in Deliverable 4.4 that are relevant for the construction of pouch cells are listed (compare Section 2.1). They are required for the calculation of the nominal capacity of the pouch cell (mass loading), for the handling during the production of the layers as well as for further processing (adhesive strength) or characterization of the binding of the active material particles via electronically and ionically conductive paths (electrical resistance, ionic conductivity, impedance). They are also required to determine the volumetric and gravimetric energy density (layer thickness, weight per unit area, nominal capacity) and thus enable an economic classification of the cell.

Table 1: Properties of final separators and cathodes (reported in D4.4).

Parameter	Separator		Cathode	
	Average	Deviation	Average	Deviation
Mass loading	24.62 mg cm <sup>-2</sup>	0.60 mg cm <sup>-2</sup>	18.39 mg cm <sup>-2</sup>	1.28 mg cm <sup>-2</sup>
Thickness (uncompacted)	249.70 μm	8.51 μm	108.90 μm	2.42 μm
Thickness (compacted)	181.00 μm	8.29 μm	87.30 μm	3.30 μm
Porosity (uncompacted)	0.44	---	0.56	---
Porosity (compacted)	0.23	---	0.45	---
Adhesive strength	0.391 MPa	0.049 MPa	0.589 MPa	0.054 MPa
Electric resistivity	---	---	764.81 Ω cm	30.68 Ω cm

Ionic conductivity	0.194 mS cm <sup>-1</sup>	0.056 mS cm <sup>-1</sup>	---	---
Impedance	---	---	23.82 Ω cm	4.92 Ω cm

Table 2 compares the specific capacity of the cells in PTFE (D4.4, circular samples of 16 mm diameter) and pouch cell construction (this deliverable). The reduction in capacity of about 80 % for the pouch cell compared to the 16 mm samples is clearly evident. Probable reasons discussed were the lower pressure during compression as well as during cycling and charge rate accuracy of the cathode. Independently of the cell assembly, the high thicknesses of separator have to be reduced. They provide long ion and electron conduction paths and thus high resistances, which might have a negative impact on cell performance. Nevertheless, the electrochemical characterization in WP6 will deliver more detailed results on this question and allow an in-depth analysis.

Table 2: Specific capacity for PTFE- and Pouch Cell Setup

Cycle	PTFE Cell (D4.4)		Pouch Cell	
	Capacity / mAh g <sup>-1</sup>	Deviation / mAh g <sup>-1</sup>	Capacity / mAh g <sup>-1</sup>	Deviation / mAh g <sup>-1</sup>
1 <sup>st</sup>	112.19	14.18	23.33	4.19
3 <sup>rd</sup>	74.70	19.47	13.66	2.56
5 <sup>th</sup>	57.34	17.01	11.61	2.66

The apparently very low active material utilization of the cells makes necessary to improve both the measurement parameters and electrode constitution. In order to be able to make improvements in a short time horizon, i. e. the next weeks, the already fabricated layers will be measured at higher temperatures. The higher temperature should result in a higher ionic conductivity of the solid electrolyte and thus better ionic contacting of the active material particles. Furthermore, the existing layers can be processed with different, possibly higher, densification parameters on the calender, which should further reduce the materials' porosity, improve the electronic and ionic conductivity and thus the contacting of the active material particles. The layer thickness would also be reduced in this way, which would positively influence the volumetric energy density.

On a longer time scale, e.g. over the next months, further changes should be made on process level, i.e. dispersion and coating process: Reducing the separator coating thickness would reduce the amount of inactive material and therefore increase the gravimetric and volumetric energy density of the cell. Also, the influence of initial fabrication pressure and stack pressure during cycling should be investigated. Although the pressure carried out by a hydraulic press respectively a calender is not directly comparable to each other, experiences from other projects with similar chemistries show much lower porosities and therefore better cell performances by using the calender. In addition, further cycling routines should be developed and included in future electrochemical investigations. Besides the process optimization, the use of improved materials should account for increased electrochemical performance: in the consortium, enhanced cathode and electrolyte materials have been announced. While the new cathode material should ensure a higher utilization during discharge and therefore a higher discharge capacity, it should also prevent side reactions with the active material. The improved sulfide electrolyte, on the other hand, should provide for a higher ionic conductivity in both separator and cathode layers, therefore increasing the active material utilization.

## 4 Risk register

Table 3: Risk Register

Risk No.	What is the risk	Probability of risk occurrence <sup>4</sup>	Effect of risk <sup>5</sup>	Solutions to overcome the risk
WP4.4	Insufficient porosity decrease during manufacturing compaction of cathodes and separator layers	1	1	Increase pressure during compaction
WP4.4	Components disintegrate during die-cutting	2	2	Decrease pressure or use additional cover material
WP4.4	Insufficient contact between electrode current collector and tab	2	2	Use ultrasonic welding to attain an electrical contact
WP4.4	Cathode and anode misalignment	2	2	Assure a correct alignment during assembly, e.g. fix the components or use a plastic mould
WP4.4	Insufficient contact between components during cycling	1	1	Increase external pressure
WP4.4	Risk of short circuit due to deteriorated components	2	1	Improve electrode quality
WP4.4	Untight pouch cells	3	2	Use a longer program for sealing or a different pouch bag material

<sup>4</sup> Probability risk will occur: 1 = high, 2 = medium, 3 = low

<sup>5</sup> Effect when risk occurs: 1 = high, 2 = medium, 3 = low

## 5 Acknowledgement

The author(s) would like to thank the partners in the project for their valuable comments on previous drafts and for performing the review.

### Project partners

#	PARTICIPANT SHORT NAME	PARTNER ORGANISATION NAME	COUNTRY
1	FEV	FEV Europe GmbH	Germany
2	ABEE	AVESTA BATTERY & ENERGY ENGINEERING	Belgium
3	CICE	CENTRO DE INVESTIGACION COOPERATIVA DE ENERGIAS ALTERNATIVAS FUNDACION, CIC ENERGIGUNE FUNDAZIOA	Spain
4	FORD	FORD OTOMOTIV SANAYI ANONIM SIRKETI	Turkey
5	CRF	CENTRO RICERCHE FIAT SCPA	Italy
6	AIT	AIT AUSTRIAN INSTITUTE OF TECHNOLOGY GMBH	Austria
7	MIM	MIMI TECH GMBH	Germany
8	POL	POLITECNICO DI TORINO	Italy
9	SAFT	SAFT	France
10	SOL	RHODIA OPERATIONS	France
11	TNO	NEDERLANDSE ORGANISATIE VOOR TOEGEPAST NATUURWETENSCHAPPELIJK ONDERZOEK TNO	Netherlands
12	Fraunhofer	FRAUNHOFER GESELLSCHAFT ZUR FOERDERUNG DER ANGEWANDTEN FORSCHUNG E.V.	Germany
13	CEA	COMMISSARIAT A L ENERGIE ATOMIQUE ET AUX ENERGIES ALTERNATIVES	France
14	UMC	Umicore	Belgium
15	UNR	Uniresearch BV	Netherlands

Table 4: Project Partners



This project has received funding from the European Union's Horizon 2020 research and innovation programme under Grant Agreement no. 875028.

This publication reflects only the author's view and the Innovation and Networks Executive Agency (INEA) is not responsible for any use that may be made of the information it contains.